A 3D magnetotelluric study of the basement structure in the Mygdonian Basin (Northern Greece)

M. Gurk[1,5], M. Smirnov[2,3], A.S. Savvaidis[1], L. B. Pedersen[3] and O. Ritter[4]
[1] Institute of Engineering Seismology and Earthquake Engineering (ITSAK), Greece
[2]University of Oulu, Finland
[3]University of Uppsala, Sweden
[4]GeoForschungsZentrum Potsdam (GFZ), Germany
[5]Institut für Geophysik, Universität zu Köln, Germany

SUMMARY

During 2006 and 2007 a total number of 92 MT/GDS sites were deployed in the Mygdonian basin (Northern Greece) to gain knowledge about the basement structure by means of 2D and 3D MT data inversion and to give information about the top-of-basement depth for seismic wave propagation models. The structure of the basement is fairly well revealed by the data.

Keywords: MT, GDS, Mygdonian basin, top-of- basement, 2D inversion, 3D inversion

INTRODUCTION

The Mygdonian basin, situated between the two lakes Volvi and Lagada ca. 45 km northeast of Thessaloniki (Fig. 1&2), is a neotectonic graben structure (5 km wide) with significant seismic activity along distinct normal fault patterns (Papazachos et al., 1979; Karagianni et al., 1999; Goldsworthy et al., 2002). Fluvioterrestrial and lacustrine sediments (approximately 200-600 m thick) are overlying the basement consisting of gneiss-schists.

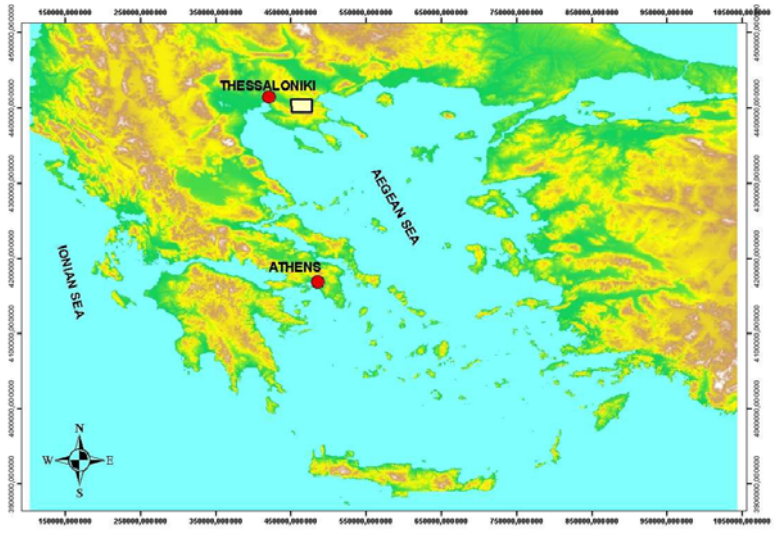

During the project "Euroseistest Volvi-Thessaloniki", a European test site for Engineering Seismology was installed in order to study velocity cross sections across the funnel shaped valley. With the actual EM survey we intend to map the top-of-basement and to contribute to seismic wave propagation modelling process and site effect assessment (Jongmans et al. 1998; Manakou et al., 2004; Savvaidis et al., 2004; Raptakis et al., 2005).

Figure 1: Map of the Aegean See with the location of the survey area (white box).

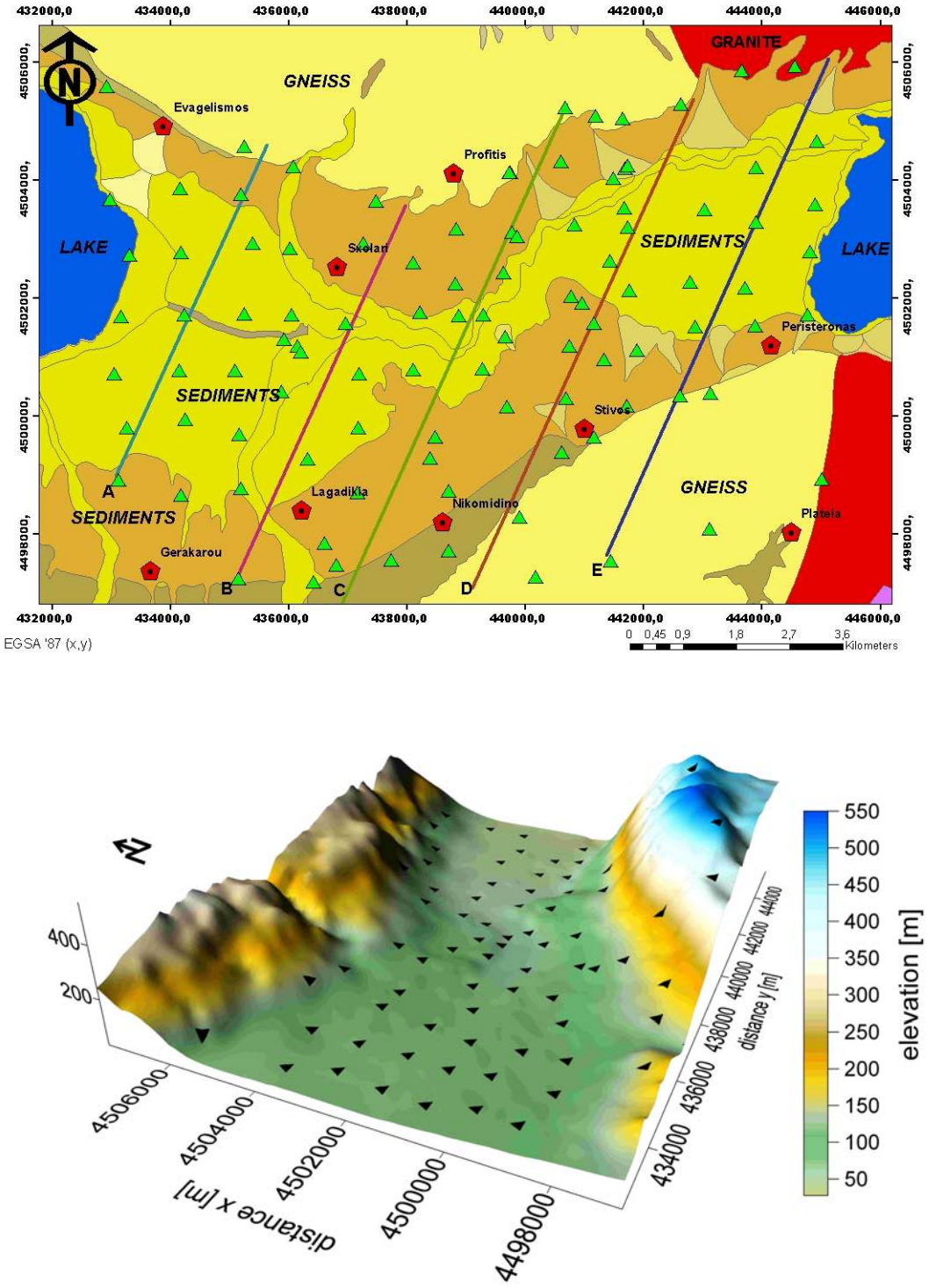

Figure 2: Map of the study area with MT site locations (triangles), Villages (red polygon), 2-D lines and geological outlines (above). Bird view towards the North-East, showing topography and MT site locations (below).

MT/GDS SURVEY

During 2006/2007 a total number of 92 MT/GDS sites were installed in the Mygdonian basin (Fig. 2). The sites were measured roughly on a regular grid (North-South and East-West) reflecting the predominant East-West orientation of many normal faults in this area. The site spacing on this grid is approximately 1 km. Some areas in the mountain and around villages are not covered due to the increased EM noise or due to inaccessibility.

MT and GDS data were collected using three MTU-2000 instruments (utilizing Earth Data PR6-24 loggers, http://www.earthdata.co.uk/prod.html) combined with Metronix MFS05 coils from Uppsala University (http://88.198.212.158/mtxweb/index.php?id=53). One of these instruments was used to collect remote reference data during the entire survey time. Due to the limited amount of induction coils, we were not able to collect the vertical magnetic field at each site. The horizontal electric field components E_x and E_y were measured with grounded non-polarisable Pb/PbCl electrodes. Where possible, the electrode spacing was extended to a maximum of 100 m using a symmetric cross shaped configuration, having the ground electrode in its centre (differential input). Generally, time series data were recorded in four frequency bands with the sampling frequencies and sample times shown in Table 1. In the following we display all spatial data in the metric Greek coordinate system EGSA-87.

	Sample frequency
Burst mode during night, 120 minutes	1 kHz
Night and day recording	20 Hz
Day recording ca. 120 minutes	3 kHz
Day recording ca. 120 minutes	120 Hz

Table 1: Sampling frequencies and recording times

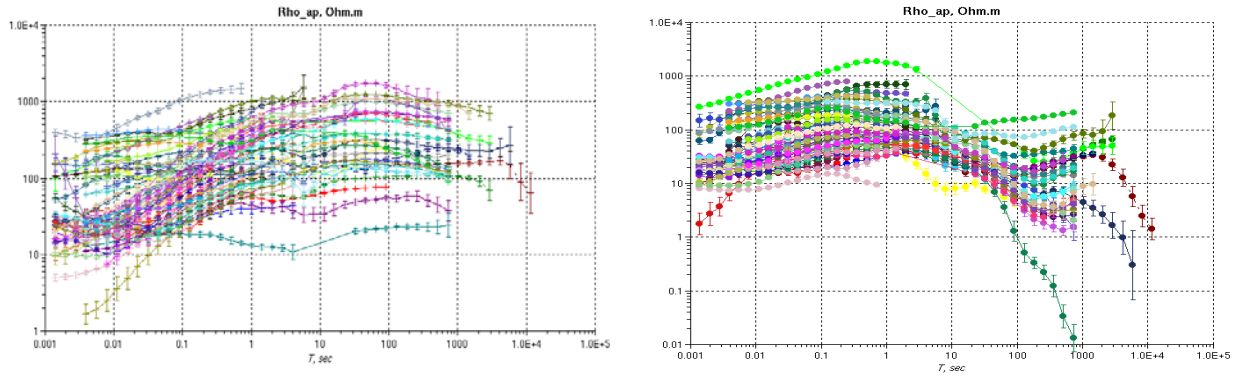

Figure 3: Unrotated apparent resistivities versus period for all sites (left: ρa-xy, right: ρa-yx).

DATA PROCESSING & ANALYSIS

Based on this survey design we obtained reliable estimates of the MT transfer function for 92 sites in the period range from T= 0.001 s to 1 s for day time recoding and from T= 0.001 s to 1000 s for the sites where both day and night recordings were available (ca. 70% of the data).
The time series were processed with the robust remote reference code of Smirnov (2003). All permutations of remote reference sites from inside and outside of the study area were used to estimate transfer functions. Also several time segments for 1 kHz and 3 kHz recordings were processed independently and thereafter averaged together with long period data to obtain the final estimates of the MT transfer functions. During robust averaging using the reduced M-estimator we calculated error bars based on bootstrap method.
Additionally, MT/GDS data were available from a 1995 survey (Savvaidis et. al., 2000; Makris et al, 2002) measured with a seven channel S.P.A.M. MkIII system (Ritter et al., 1998) coupled with Metronix MFS05 magnetic sensors. The original time series were reprocessed with the Egbert code (Egbert, 1997) using standard 128 s time windows for the distinct frequency bands. From this 1995 survey, 9 MT sites in a period range of T= 0.008 s – 100 s were used for the 2D and 3D inversion.

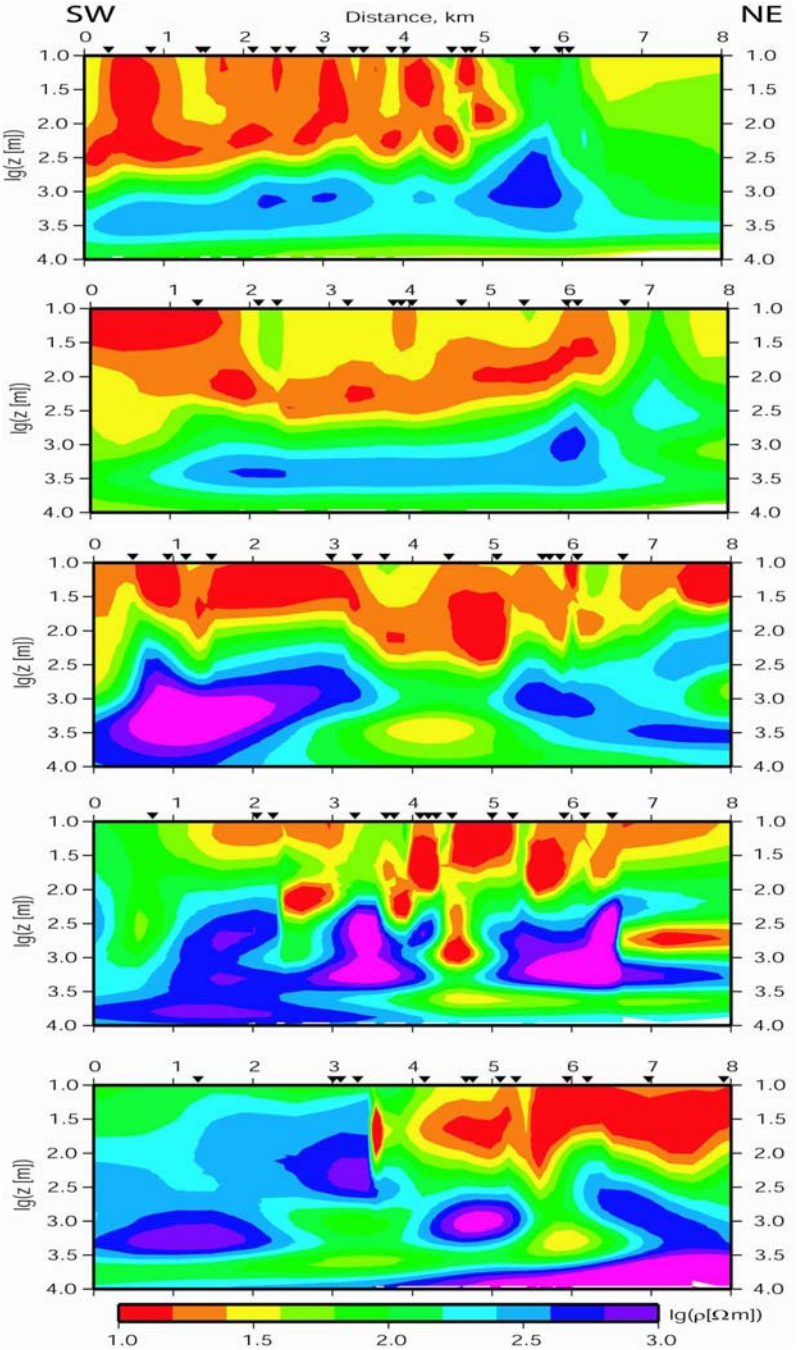

Figure 4: 2D resistivity models of line A-E (from top to bottom). Triangles indicate MT site locations.

In order to validate the 2D inversion, we carried out strike and dimensionality analysis. The strike analysis of the MT data revealed two predominant strike directions: For short periods up to ca. T= 3 s, a local strike of approximately 0° / 90 ° is found, whereas for longer periods a regional strike of about 135° / 45 ° can be deduced from the MT data. The regional and local strike is consistent with previous results of MT data from this area (Makris et al, 2002). For longer periods, real parts of induction arrows are pointing towards the South-West showing a regional strike direction of about N120°E. The overall GDS data quality from the 2006/2007 survey is poor thus we did not use them for any 2D and 3D inversion tasks. At this time this behaviour is not well understood, since GDS data from the 1995 survey (Savvaidis et. al., 2000) and a recent GDS instrument test (Gurk, pers. comm.) show good GDS results. Dimensionality parameter did not show significant 3D effects in the data, allowing us to use 2D inversion techniques.

2D INVERSION

Generally, the MT data are of good quality. However before inversion, each MT transfer function has been carefully examined. The main impedance components as well as the Berdichevsky impedance tensor determinant average data (short: Berdichevsky Invariant; Berdichevsky et. al., 1976), were tested for consistency by using 1D inversion. After this procedure, MT data from 74 sites (out of 92 measured) have been chosen for the 2D and 3D modelling.

All selected sounding curves used for this study are presented in Figure 3. The 2D inversion was performed along five parallel profiles (A-E) striking N30°E at quasi equal distances. Each MT site was then projected on the according profile. In order to perform the 2D inversion, we followed the strategy of Pedersen & Engels, (2005) inverting only Berdichevsky Invariant data. Since the Berdichevsky Invariant is by definition rotationally invariant, any variability in strike direction with period does not affect the results as much as for bi-modal inversion, when the proper mode decomposition is vital.

The 2D inversion routine by Siriponvaraporn and Egbert (2000) including the modifications made by Pedersen and Engels (2005) allow for inversion of the Berdichevsky Invariant. Error floors equal to 2% for the impedance phase (corresponding to an absolute error of 1.2°) and 50 % for the apparent resistivities were adopted. Since there was no

other information in order to constrain the static shift effect and the site spacing is relatively small, we have chosen a higher error floor for the resistivity data compared to the phases to allow the inversion procedure to have more freedom to compensate for these effects.
Finally, a homogeneous halfspace of 100 Ωm was used as the starting model for all 2D inversions. This procedure resulted in an overall good fit of the measured data to the model (RMS 1). The series of the 2D inversion results shown in Figure 4 indicate an increase in complexity of the conductivity distribution towards the East that is likely to be caused by a more complicated 3D geological setting in this part of the survey area. Hence a simplified 2D analysis of the MT transfer function can be misleading in these regions. Consequently we proceed with a 3D inversion of the data set.

3D INVERSION

The same data set, consisting of 74 pre-selected good quality MT sites, was used for the 3D inversion (Siriponvaraporn et al., 2005). Until now, the code does not account for topographic information, nor for vertical magnetic fields. Generally, MT data were measured on a more or less regular grid in the 12 km x 6 km survey area with an approximate site distance of about 1 km.
After choosing the origin of the model domain at the location of MT site a1309 it was necessary to shift the MT sites accordingly to their new position in the model domain. To get an even site distribution we allowed for relatively large lateral shifts of those sites that where measured directly on the outcropping basement rocks, e. g. in the Northern part of the area (Fig. 5). The model grid itself was designed to have 4 cells between each site. During the first inversion trial we have selected only 3 periods in the range from T= 1 s - 0.01 s. Therefore, the grid was constructed to be a 34 x 34 x 21 matrix including additional 5 horizontal outer cells to extend the grid boundaries to 60 km.

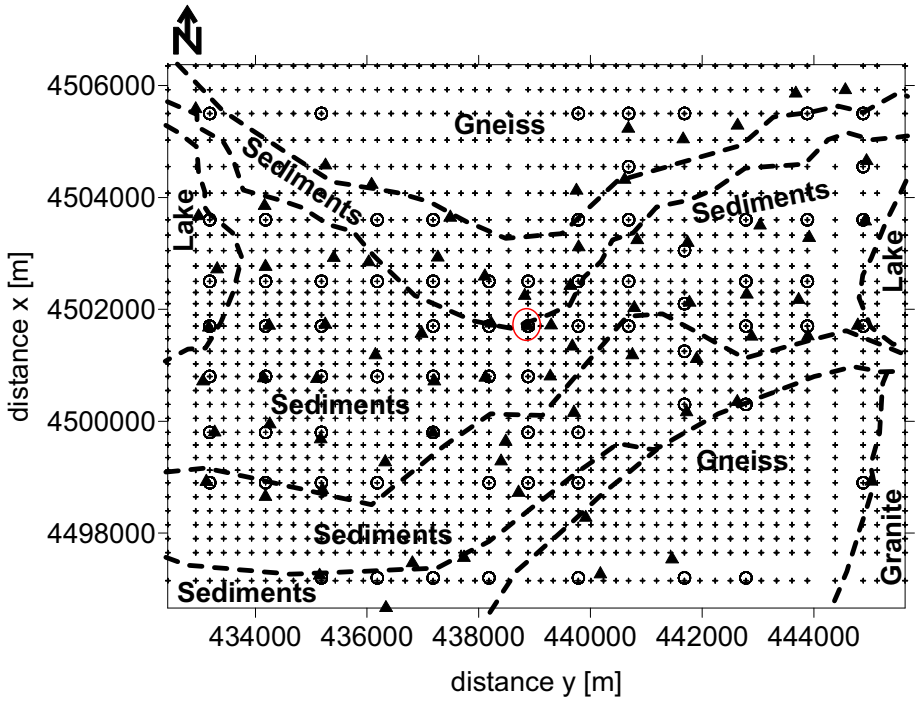

Figure 5: Plan view of the central part of the model grid (denoted as crosses) together with the MT site location (triangles), the MT site location in the model domain (circles) and geological outlines. The red circle indicates the centre of the grid.

The second inversion run included 8 periods in the range of T= 10 s– 0.01 s, using the same model grid, whereas for the third inversion the number of cells in-between sites were increased and a better vertical discrimination at target depths (42 x 54 x 26 cells) was applied. For the 3D inversion we have used the complete impedance tensor (Z_{xx}, Z_{xy}, Z_{yx} & Z_{yy}). After 4 successful iterations of the 3D routine the inversion code reached RMS values of approximately 10.

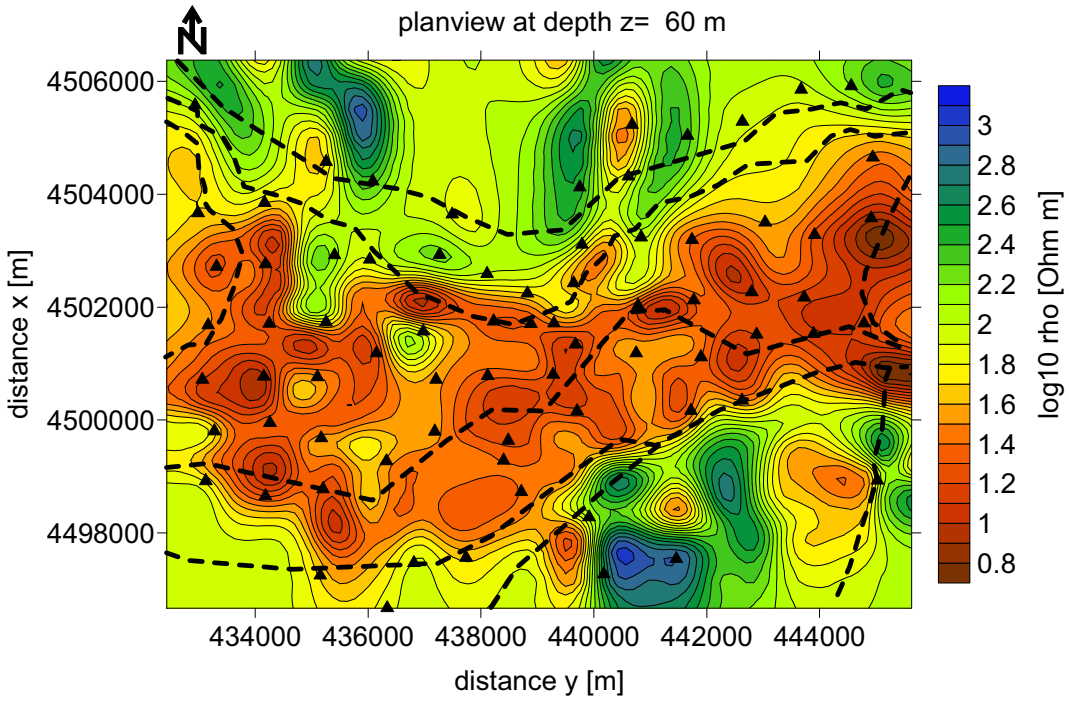
planview at depth z= 60 m
N
4506000
4504000
4502000
4500000
4498000
distance x [m]
434000
436000
438000
440000
442000
444000
distance y [m]
3
2.8
2.6
2.4
2.2
2
1.8
1.6
1.4
1.2
1
0.8
log10 rho [Ohm m]

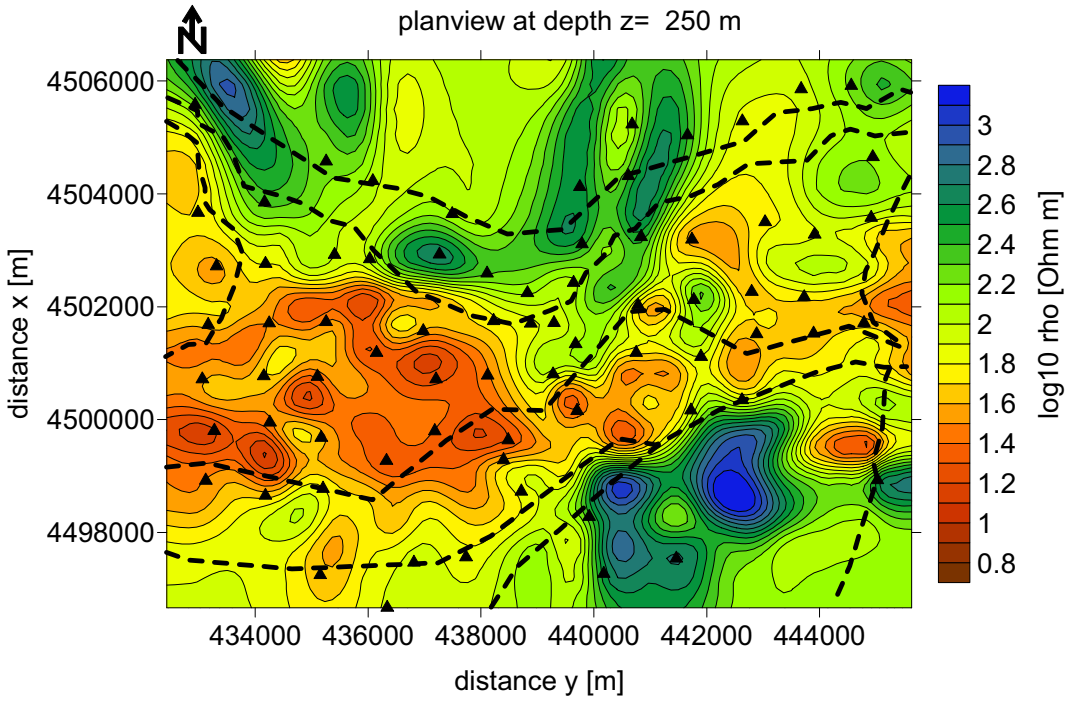
planview at depth z= 250 m
N
4506000
4504000
4502000
4500000
4498000
distance x [m]
434000
436000
438000
440000
442000
444000
distance y [m]
3
2.8
2.6
2.4
2.2
2
1.8
1.6
1.4
1.2
1
0.8
log10 rho [Ohm m]

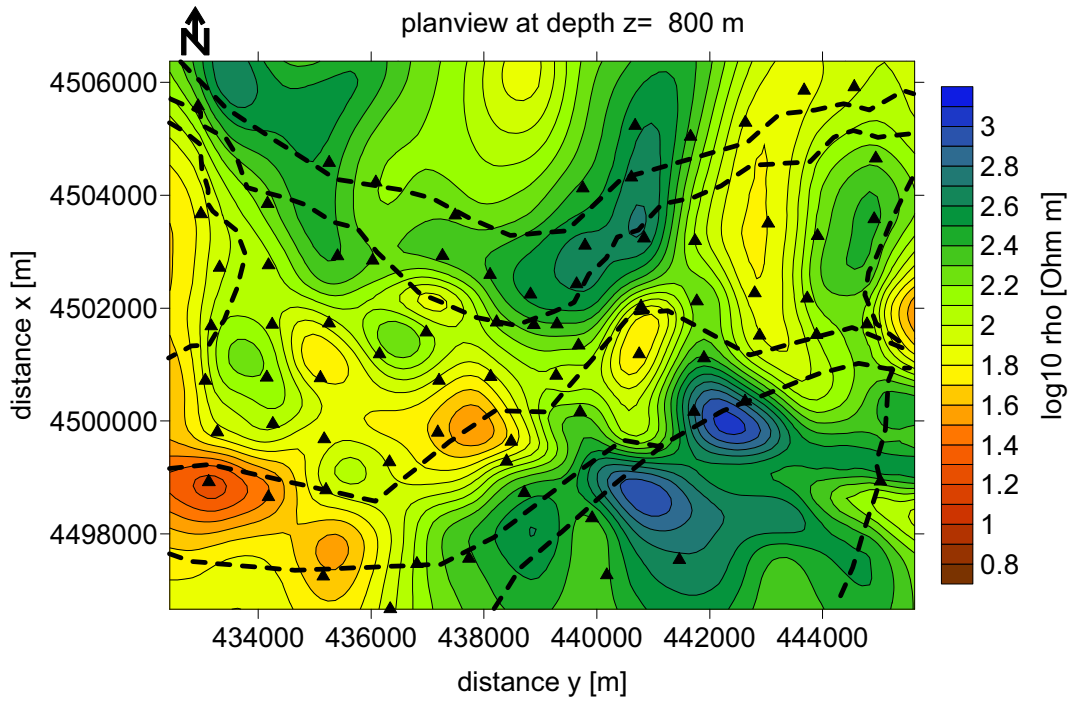

Figure 6: Plan view of 3D resistivity models at three different depths (triangles indicate MT site locations, hashed lines indicate geological boundaries).

Figure 6 shows representative examples of the 3D inversion results of our last run as plain view at three different depths. The resistivity of the lacustrine sediments (approx. 40 Ωm) in the valley contrasts clearly with the higher resistivities of the surrounding basement rocks allowing to map the structures at near surface (z = 60 m) in very good accordance to the geological setting as displayed in Figure 2. In a larger depth range at z= 250 m, the influence of a basement high is more pronounced towards the centre of the area. The sediments (approx. 40-60 Ωm) in the Eastern part of the area seem to vanish whereas in the Western part sediments are still visible. At a depth of z= 800 m only sediments in the South Western part of the valley are still recognisable, the basement high in the middle of the valley is now fully developed and the sediments towards the East are not pronounced any more.

The normalised absolute misfit of the real part of the impedance tensor elements Z_{xy} and Z_{yx} are shown in Figure 7. The data misfit is higher in the Western part of the area than compared to the Eastern part, which is in agreement to the previous 2D model study. Large misfits can be found where the MT site distribution and/or data quality is poor. It is a striking feature in Figure 6 that the misfit follows the topography or morphology of the survey area which could mean that static shift and/or topographic effects may play a more important role in the error distribution than previously considered. Hence the entire data set should be re-analysed more carefully with respect to galvanic distortion models.

3D MODEL VOLUME

The 3D inversion results at distinct depth values can be presented using volume rendering tools. Since our task is to map the top-of-basement by means of an iso-resistivity layer, we have to confine the range of resistivity values that can be associated with the top-of-basement rocks. Due to the changing hydrogeological conditions which leads to different degrees of weathering of the basement rocks, it is not possible to allocate a unique resistivity value to the top–of-basement. Nevertheless, we can use available information from boreholes and VES data (Euroseistest, 1995; Tournas, 2005) to constrain the resistivity range and the depth to the basement rocks at specific locations. Our first approach is displayed in Figure 8 to highlight the onset of the basement resistivities, indicated by the transition between yellow and green colors (approx. 75 Ωm). From these considerations a 90 Ωm iso-surface can be deduced that matches sufficiently to basement information from boreholes (see Fig. 9). Studying the conductivity distribution in general with in the 3D

volume, we see that the sediments with the lowest resistivities can be found in a band along the Southern rim of the valley. Towards the North, the resistivities of the sediments increase gradually.

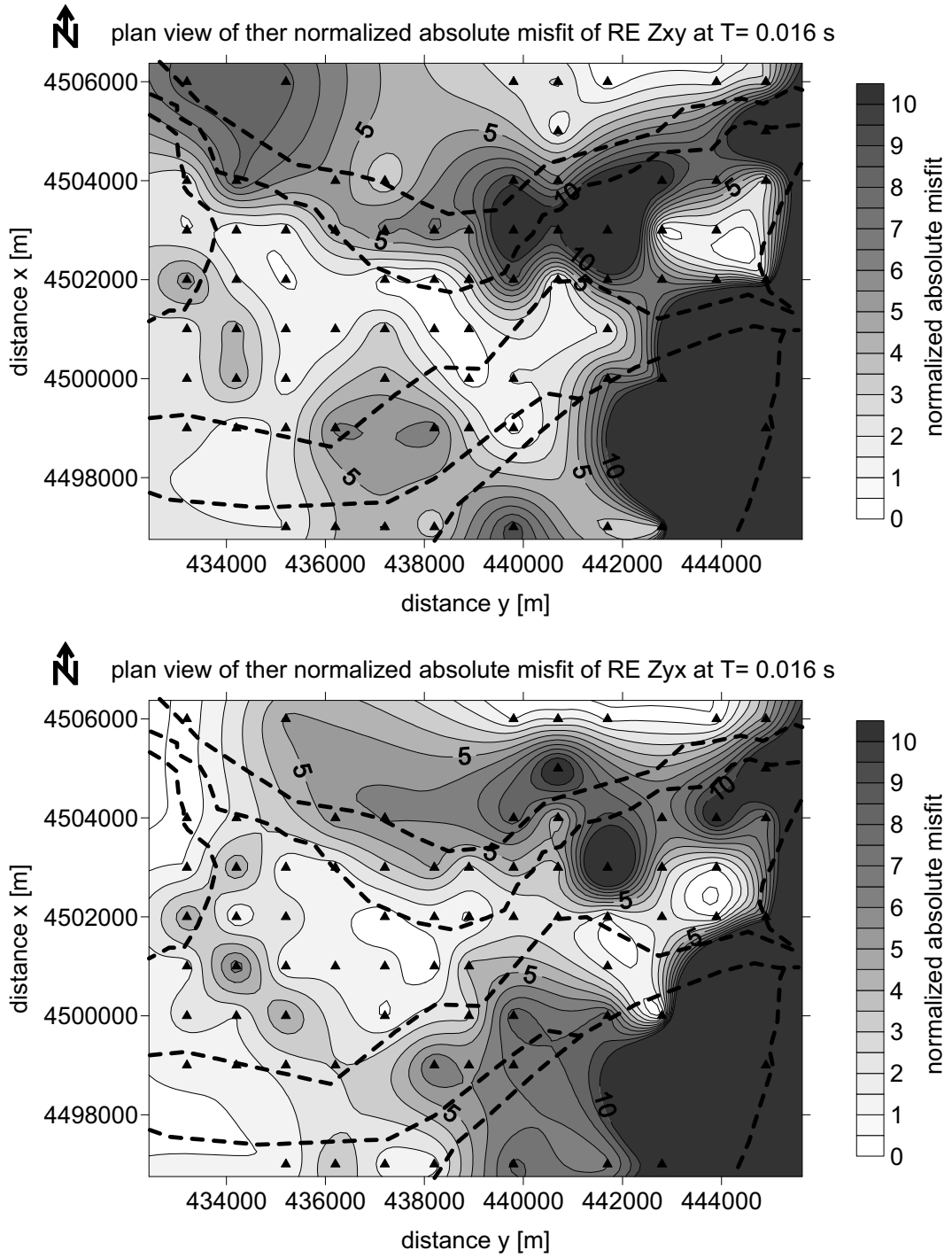

Figure 7: Plan view of the normalized absolute misfit at T= 0.016 s for the real part of the impedance tensor elements Z_{xy} (up) and Z_{yx} (below). Triangles indicate MT site locations, hashed lines indicate geological boundaries.

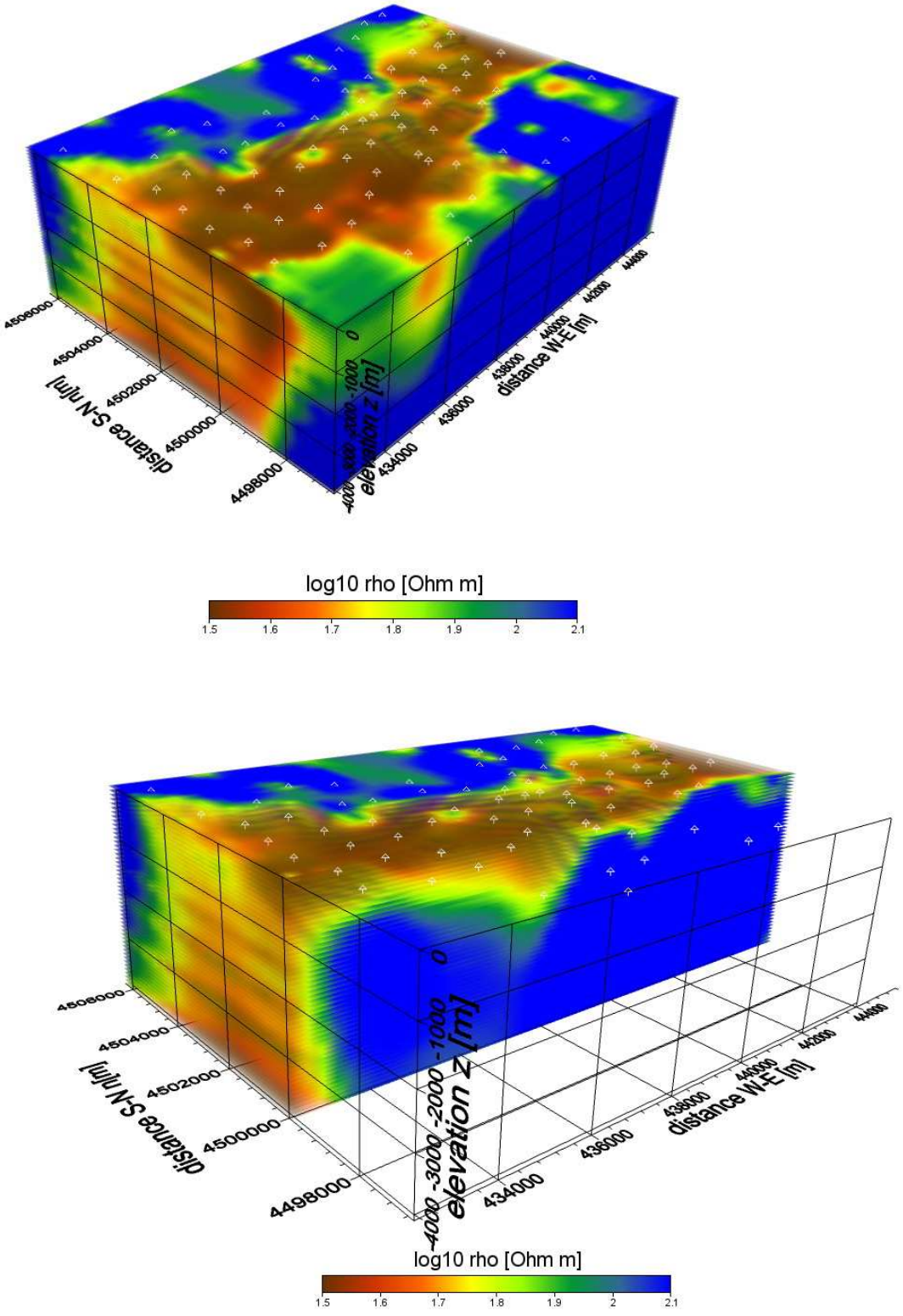

Figure 8: Two 3D bird views of the resistivity model in North-East direction. Triangles indicate MT sites.

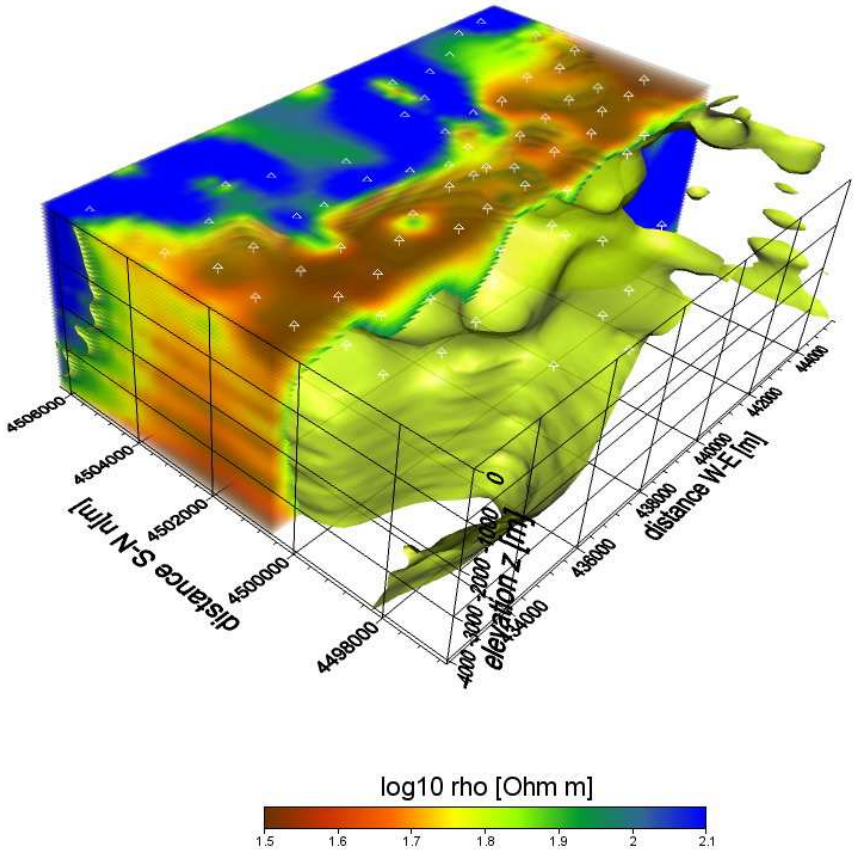

Figure 9: 3D view of the top of basement (90 Ω m iso-surface, green color) in North-East direction. Triangles indicate MT sites.

CONCLUSIONS

MT array data were used to obtain new information about the sediment thickness and the slope of the top-of-basement in the South-Eastern part of the investigation area which is of particular importance for seismic wave propagation modeling. To support this finding in our future work new MT sites are going to be deployed to stretch the 2D sections A, B and C towards the South-East. In the next inversion attempt, we pay more attention to galvanic and topographic effects, as well as to confine the model results with available VES and RMT/CSTAMT information.

ACKNOWLEDGEMENTS

This study is supported by the project of the Marie Curie Action ITSAK-GR (International Transfer of Seismological Advanced Knowledge – Geophysical Research), MTCD-CT-2005-029627. We are greatly indebted to the students from Thessaloniki and Crete who took part in the fieldwork. Finally we would like to thank Lars Dynesius for all his technical help and support during the field measurements.

REFERENCES

Berdichevsky, M.N. and Dmitriev, V.I., (1976), Basic principles of interpretation of magnetotelluric sounding curves, *in Adam A., Ed., Geoelectric and geothermal studies*: Budapest, Akamdemai Kiado, 165-221.

Egbert, G.D. (1996). Robust Multiple-Station Magnetotelluric Data Processing, *Geophys. J. Int.,* 130, 475–496.

EUROSEISTEST, (1995): 'Volvi-Thessaloniki: A European Test Site for Engineering Seismology, Earthquake Engineering & Seismology', Final Scientific Report, October 1995.

Goldsworthy, M., J. Jackson and J. Haines (2002) . The continuity of active fault systems in Greece, *Geophys. J. Int.,* 148, 596–618.

Jongmans,D., Pitilakis, K., Demanet, D., Raptakis, D., Hor-rent, C., Tsokas, G., Lontzetidis, K., Riepl, J., (1998). EURO-SEISTEST: Determination of the Geological Structure of the Volvi Graben and validation of the basin response to one earthquake and one shot. Bull. Seismol. Soc. Am. 88, 473–487.

Karagianni, E.E., D.G. Panagiotopoulos, C.B. Papazachos, and P.W. Burton (1999). A study of shallow crustal structure in the Mygdonia Basin (N. Greece) based on the dispersion curves of Rayleigh waves. *Journal of the Balkan Geophysical Society*, Vol. 2, No 1, 3-14.

Manakou M. Raptakis D., Chavez-Garcia F., Makra K., Apostolidis P. Pitilakis K., (2004), Construction of the 3D geological structure of Mygdonian basin (N. Greece), in proceedings of: 5th International Symposium on eastern Mediterranean Geology, Thessaloniki, Greece, 14-20. April, Ref: S6-15

Makris J. P., Savvaidis, A. and Valliantos, F. (2002). MT-data analysis from a survey in the Mygdonian basin (N. Greece). *Anals of Geophysics* 45, 303-311.

Papazachos, B.C., Mountrakis, D., Psilovikos, A., and Leventakis, G., (1979). Surface fault traces and fault plane solutions of the May-June 1978 major shocks in the Thessaloniki area, Greece, Tectonophysics, 53, 171-183

Pedersen, L.B. and Engels, M. (2005). Routine 2D inversion of Magnetotelluric data using the determinant of the impedance tensor. *Geophysics* 70, G33-G41.

Raptakis D., Manakou M., Chavez-Garcia F., Makra K., Pitilakis K., (2005), 3D configuration of Mygdonian basin and preliminary estimate of its site response, Soil dynamics and Earthquake Engineering, 25, 871-887.

Ritter, O., Junge, A., Graham, J., Dawes K., (1998). New equipment and processing for magnetotelluric remote reference observations. Geophys. J. Int, 132, 535-548.

Savvaidis, A. Pedersen, L. B., Tsokas, G. N., Dawes, G. J., (2000). Structure of the Mygdonian Basin (N. Greece) inferred from MT and gravity data, *Tectonophysics*, 317, 171-186.

Savvaidis A., Theodoulidis N., Panou A., Papazachos C. and Hatzidimitriou P., (2004). Geophysical Information from Ambient Noise Data in the Volvi Basin, 10th Congress of the Geological Society of Greece, Thessaloniki, Greece, 15 - 17 April 2004.

Siripunvaraporn W. and Egbert G, (2000**).** An efficient data-subspace inversion method for 2-D magnetotelluric data. *Geophysics*, 65, 791–803.

Siripunvaraporn W., G. Egbert, Y. Lenbury and M. Uyeshima. (2005). Three-Dimensional Magnetotelluric: Data Space Method, *Physics of the Earth and Planetary Interiors*, 150, 3-14.

Smirnov, M., (2003). Magnetotelluric data processing with a robust statistical procedure having a high breakdown point, *Geophys.J.Int*., 152, 1-7.

Tournas, D., (2005). Study of the geometry of the Mygdonian Basin in the area of the European Test Site with Geophysical Methods, *MSc, Aristotle University, Thessaloniki (in Greek)*. pp. 145.